

# Technical Notes

TECHNICAL NOTES are short manuscripts describing new developments or important results of a preliminary nature. These Notes should not exceed 2500 words (where a figure or table counts as 200 words). Following informal review by the Editors, they may be published within a few months of the date of receipt. Style requirements are the same as for regular contributions (see inside back cover).

## Three-Dimensional Transient Radiative Transfer Modeling Using Discontinuous Spectral Element Method

J. M. Zhao\* and L. H. Liu†

Harbin Institute of Technology, 150001 Harbin, People's Republic of China

DOI: 10.2514/1.39361

### Nomenclature

$A$	=	area, $\text{m}^2$
$a$	=	anisotropy parameter of linear anisotropic-scattering phase function
$c$	=	speed of light, $\text{m/s}$
$G$	=	integrated intensity, as defined by Eq. (8a), $\text{W/m}^2$
$\mathbf{H}$	=	matrix, as defined in Eq. (7)
$h$	=	one-dimensional standard nodal basis function
$\tilde{h}$	=	three-dimensional standard nodal basis function
$I$	=	radiative intensity, $\text{W}/(\text{m}^2 \cdot \text{sr})$
$I_b$	=	blackbody radiative intensity, $\text{W}/(\text{m}^2 \cdot \text{sr})$
$I_p$	=	transient intensity on the boundary, $\text{W}/(\text{m}^2 \cdot \text{sr})$
$I_0$	=	amplitude of transient intensity, $\text{W}/(\text{m}^2 \cdot \text{sr})$
$K$	=	general hexahedral element
$K_{\text{st}}$	=	standard hexahedral element
$\mathbf{k}$	=	unit direction vector of $z$ direction
$L_R$	=	reference length scale, $\text{m}$
$\mathbf{M}$	=	matrix, as defined in Eq. (7)
$M$	=	number of discrete-ordinate directions
$N_{sk}$	=	number of solution nodes on each element
$N_t$	=	number of discretized time steps
$N_\theta$	=	number of subdivisions for a zenith angle
$N_\varphi$	=	number of subdivisions for an azimuthal angle
$\mathbf{n}_w$	=	unit normal vector of the wall
$\mathbf{n}_{\partial K}$	=	unit normal vector at the boundary of element $K$
$p$	=	order of polynomial expansion
$q_z$	=	heat flux of $z$ direction, as defined by Eq. (8b), $\text{W/m}^2$
$\mathbf{r}$	=	vector of spatial coordinates $(x, y, z)$
$\tilde{S}$	=	function, as defined in Eq. (7d), $\text{W/m}^3$
$T$	=	temperature, $\text{K}$
$t$	=	time, $\text{s}$
$t^*$	=	dimensionless time $ct/L_R$ , dimensionless time step
$u$	=	unit step function

$V$	=	volume, $\text{m}^3$
$w$	=	weight of discrete-ordinates approximation, $\text{sr}$
$x, y, z$	=	global coordinate system variables
$\mathbf{x}_{\text{st}}$	=	local coordinate vector $(x_{\text{st}}, y_{\text{st}}, z_{\text{st}})$
$x_{\text{st}}, y_{\text{st}}, z_{\text{st}}$	=	reference coordinate system variables
$\beta$	=	extinction coefficient $(\kappa_a + \kappa_s)$ , $\text{m}^{-1}$
$\beta$	=	function, as defined in Eq. (7c), $\text{m}^{-1}$
$\Delta t^*$	=	dimensionless time step
$\theta$	=	zenith angle
$\kappa_a$	=	absorption coefficient, scattering coefficient, $\text{m}^{-1}$
$\kappa_s$	=	scattering coefficient, $\text{m}^{-1}$
$\rho$	=	bidirectional reflection function
$\sigma$	=	Stefan–Boltzmann constant, $\text{W}/(\text{m}^2 \cdot \text{K}^4)$
$\tau_L$	=	optical thickness, $\beta L$
$\tau_p$	=	transmissivity
$\Phi$	=	scattering phase function
$\phi$	=	global nodal basis function
$\varphi$	=	azimuthal angle
$\psi$	=	map function, as defined by Eq. (5)
$\Omega$	=	solid angle, $\text{sr}$
$\mathbf{\Omega}$	=	unit vector of the radiation direction
$\omega$	=	single scattering albedo

### Subscripts

$i$	=	mapped one-dimensional index
$i', j', k'$	=	elemental spatial node index
$l$	=	node index of the standard hexahedral element
$n$	=	time step index
$w$	=	value at wall

### Superscripts

$m, m'$	=	index of discrete-ordinate direction
---------	---	--------------------------------------

## I. Introduction

TRANSIENT radiative transfer within a participating medium has attracted the interest of many researchers due to the availability of short-pulse lasers and their application to many emerging new technologies [1–3]. A number of methods have been developed to solve the transient radiative transfer equation (TRTE); such as the Monte Carlo method [4], the integral equation method [5], the discrete-ordinates method (DOM) [6,7], and the finite volume method (FVM) [8]. Among them, the methods based on the differential form of the TRTE, such as the DOM and the FVM, are efficient and easy to apply to problems with complex media and boundary conditions. However, the DOM and the FVM suffer from large false scattering, and the transient wave front cannot be captured efficiently and accurately.

Recently, based on a discontinuous Galerkin (DG) approach, Liu and Hsu [9] developed and analyzed transient radiative transfer in two-dimensional graded index media using a discontinuous finite element method (DFEM). In the DG approach, the approximation space is composed of discontinuous functions, which is expected to be ideal in solving transient radiative transfer problems and accurately capturing the sharp wave fronts. The DFEM showed good performance in solving the transient radiative transfer problems. As an advanced version of the DFEM, a discontinuous spectral element

Received 26 June 2008; revision received 18 June 2009; accepted for publication 18 June 2009. Copyright © 2009 by the American Institute of Aeronautics and Astronautics, Inc. All rights reserved. Copies of this paper may be made for personal or internal use, on condition that the copier pay the \$10.00 per-copy fee to the Copyright Clearance Center, Inc., 222 Rosewood Drive, Danvers, MA 01923; include the code 0887-8722/09 and \$10.00 in correspondence with the CCC.

\*Ph.D., School of Energy Science and Engineering, 92 West Dazhi Street; jzmhaocn@gmail.com.

†Professor, School of Energy Science and Engineering, 92 West Dazhi Street; lhliu@hit.edu.cn (Corresponding Author).

method (DSEM) [10] that enriches the DFEM due to the high-order accuracy of the spectral method, was developed to solve transient radiative transfer problems. The DSEM was shown to be efficient and accurate in capturing the sharp wave front of the transient radiative transfer process. However, performance of the DSEM has only been examined in one- and two-dimensional cases.

In this note, the DSEM is formulated and applied to solve the three-dimensional transient radiative transfer problems. Its performance in solving three-dimensional transient radiative transfer is studied and verified.

## II. Transient Radiative Transfer Equation

The discrete-ordinates form of the TRTE for an absorbing, nonemitting, and scattering medium can be written as [11]

$$\begin{aligned} \frac{\partial I^m(\mathbf{r}, t)}{c \partial t} + \boldsymbol{\Omega}^m \cdot \nabla I^m(\mathbf{r}, t) + \beta I^m(\mathbf{r}, t) \\ = \frac{\kappa_s}{4\pi} \sum_{m'=1}^M I^{m'}(\mathbf{r}) \Phi(\boldsymbol{\Omega}^m, \boldsymbol{\Omega}^{m'}) w^{m'} \end{aligned} \quad (1a)$$

with the boundary condition and initial condition given as [11]

$$\begin{aligned} I^m(\mathbf{r}_w, t) = I_p(\mathbf{r}_w, \boldsymbol{\Omega}^m, t) \tau_p(\mathbf{r}_w, \boldsymbol{\Omega}^m) \\ + \sum_{\mathbf{n}_w \cdot \boldsymbol{\Omega}^{m'} < 0} \rho(\mathbf{r}_w, \boldsymbol{\Omega}^m, \boldsymbol{\Omega}^{m'}) I_{w'}^{m'} | \mathbf{n}_w \cdot \boldsymbol{\Omega}^{m'} | w^{m'} \\ \mathbf{n}_w \cdot \boldsymbol{\Omega} < 0 \end{aligned} \quad (1b)$$

$$I(\mathbf{r}, \boldsymbol{\Omega}, t) = 0, \quad t = 0 \quad (1c)$$

The DSEM is then developed, based on Eqs. (1), to model transient radiative transfer processes.

## III. Discontinuous Spectral Element Method Discretization

The radiative intensity field of the  $n$ th time step and direction  $\boldsymbol{\Omega}^m$  is approximated in a function space spanned by Chebyshev nodal basis functions defined on an element  $K$  as [10]

$$I_n^m(\mathbf{r}) \simeq \sum_{i=1}^{N_{sk}} I_{n,i}^m \phi_i(\mathbf{r}) \quad (2)$$

where  $I_{n,i}^m$  denotes the radiative intensity of the  $i$ th node and  $\phi_i$  is the nodal basis function of node  $i$  defined on  $K$ . In the present study, the solution domain is subdivided into hexahedral elements. The standard element  $K_{st}$ , defined in the reference coordinate system as shown in Fig. 1, is a cube:

$$K_{st}: x_{st}, y_{st}, z_{st} \in [-1, 1]$$

The three-dimensional nodal basis function defined on  $K_{st}$  is formulated as

$$\begin{aligned} \hat{h}_i(x_{st}, y_{st}, z_{st}) = h_{i'}(x_{st}) h_{j'}(y_{st}) h_{k'}(z_{st}) \\ i', j', k' = 1, \dots, p+1, \quad i = 1, \dots, (p+1)^3 \end{aligned} \quad (3)$$

where  $h_{i'}$  is the one-dimensional Chebyshev nodal basis function defined on  $[-1, 1]$  [12] and  $i$  is an index map defined as

$$i = i(i', j', k') = i' + (j' - 1)(p + 1) + (k' - 1)(p + 1)$$

and  $p$  is the order of the Chebyshev polynomial expansion.

The elemental nodal basis function  $\phi_i(x, y, z)$ , defined on a general hexahedron element  $K$ , can be obtained from the reference basis function  $\hat{h}_i(x_{st}, y_{st}, z_{st})$  defined on the standard element  $K_{st}$  using a coordinate transformation, as depicted in Fig. 1. The coordinate transformation is defined based on the coordinates of the eight vertices of  $K_{st}$  ( $\mathbf{x}_{st,l}$ ,  $l = 1, \dots, 8$ ), as shown in Fig. 1, and the corresponding coordinates of the eight vertices of  $K$  and  $\mathbf{r}_l$  as

$$\begin{aligned} \mathbf{r}(\mathbf{x}_{st}) = \sum_{l=1}^8 \mathbf{r}_l \psi_l(\mathbf{x}_{st}), \quad \mathbf{r} = (x, y, z) \in K \\ \mathbf{x}_{st} = (x_{st}, y_{st}, z_{st}) \in K_{st} \end{aligned} \quad (4)$$

where  $\psi_l$  is a mapping function related to the vertex  $\mathbf{x}_{st,l}$  that is defined as

$$\begin{aligned} \psi_l(\mathbf{x}_{st}) = \frac{1}{8} [1 + \text{sign}(x_{st,l}) x_{st}] [1 + \text{sign}(y_{st,l}) y_{st}] [1 + \text{sign}(z_{st,l}) z_{st}] \\ l = 1, \dots, 8 \end{aligned} \quad (5)$$

Then,  $\phi_i(x, y, z)$  is obtained from  $\hat{h}_i(x_{st}, y_{st}, z_{st})$  as

$$\phi_i(\mathbf{r}) = \phi_i[\mathbf{r}(\mathbf{x}_{st})] = \hat{h}_i(\mathbf{x}_{st}), \quad \mathbf{r} \in K, \quad \mathbf{x}_{st} \in K_{st} \quad (6)$$

By substituting the three-dimensional spectral approximation of the intensity field [Eq. (2)] into the TRTE Eqs. (1)] and following the general discontinuous Galerkin approach outlined in the preceding work [10,13], the final DSEM discretization of Eqs. (1) over element  $K$  at the  $n$ th time step is obtained as

$$\mathbf{M}_n^m \mathbf{I}_n^m = \mathbf{H}_n^m, \quad n = 1, \dots, N_t \quad (7a)$$

where the matrices  $\mathbf{M}_n^m$  and  $\mathbf{H}_n^m$  are defined, respectively, as

$$\begin{aligned} M_{n,ji}^m = - \int_K \phi_i \boldsymbol{\Omega}^m \cdot \nabla \phi_j dV + \frac{1}{2} \int_{\partial K} (\boldsymbol{\Omega}^m \cdot \mathbf{n}_{\partial K} + |\boldsymbol{\Omega}^m|) \phi_i \phi_j dA \\ + \int_K \tilde{\beta}_n \phi_i \phi_j dV \end{aligned} \quad (7b)$$

$$H_{n,ji}^m = \int_K \tilde{S}_n^m \phi_j dV - \frac{1}{2} \int_{\partial K} (\boldsymbol{\Omega}^m \cdot \mathbf{n}_{\partial K} - |\boldsymbol{\Omega}^m|) I_{n,-}^m \phi_j dA \quad (7c)$$

where the superscript operator  $-$  denotes the values at the outside of element  $K$  [10], in which  $\tilde{\beta}_n$  and  $\tilde{S}_n(\mathbf{r}, \boldsymbol{\Omega})$  are defined, respectively, as

$$\tilde{\beta}_n = \frac{2}{L_R \Delta t^*} + \beta \quad (7d)$$

$$\begin{aligned} \tilde{S}_n^m(\mathbf{r}) = \frac{\kappa_s}{4\pi} \sum_{m'=1}^M [I_{n,i}^{m'}(\mathbf{r}) + I_{n-1,i}^{m'}(\mathbf{r})] \Phi(\boldsymbol{\Omega}^m, \boldsymbol{\Omega}^{m'}) w^{m'} - \boldsymbol{\Omega}^m \\ \cdot \nabla I_{n-1,i}^m(\mathbf{r}) - \left[ \beta - \frac{2}{L_R \Delta t^*} \right] I_{n-1,i}^m(\mathbf{r}) \end{aligned} \quad (7e)$$

where  $L_R$  is a reference length and is selected as the characteristic length of the problem,  $t^* = ct/L_R$  is dimensionless time and  $\Delta t^*$  is the dimensionless time step. The matrix equations given by Eqs. (7) are solved element by element, at each time step, through Gaussian elimination.

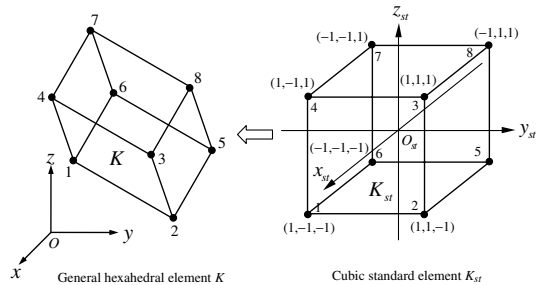


**Fig. 1** Schematic of coordinate transformation from  $K_{st}$  (defined in the reference coordinate system  $x_{st}, y_{st}, z_{st}$ ) to  $K$  (in the global coordinate system  $x, y, z$ ).

**Table 1** Boundary condition and medium property for different cases

Case	Bottom boundary, $z = 0^a$	Medium property	Other boundaries
1	Diffuse emission, $I_p = I_0 u(t)$ , $I_0 = 1 \text{ W/m}^2 \cdot \text{sr}$	Isotropic scattering, $\tau_L = 1$ , $\omega = 0.1$	Transparent, nonreflective
2	Diffuse emission, $I_p = I_0 u(t)$ , $I_0 = 1 \text{ W/m}^2 \cdot \text{sr}$	Linear anisotropic scattering: $\Phi = 1 + a \mathbf{\Omega} \cdot \mathbf{\Omega}'$ , $\tau_L = 1$ , $\omega = 1$ , $a = -1, 0, 1$	Transparent, nonreflective
3	Collimated intensity in $z$ direction, $I_p = I_0 u(t) \delta(\mathbf{\Omega} - \mathbf{k})$ , $I_0 = 1 \text{ W/m}^2 \cdot \text{sr}$	Isotropic scattering, $\tau_L = 0.1, 1, 2$ , $\omega = 1$	Transparent, nonreflective

<sup>a</sup>Here,  $u(t)$  is the unit step function, which is unity for  $t > 0$ , and zero otherwise;  $\mathbf{k}$  is the unit direction vector of the  $z$  direction.

#### IV. Results and Discussion

The DSEM described previously is applied to solve the transient radiative transfer problem in a cubic medium of side length  $L$  for the boundary-driven problems listed in Table 1. As for a numerical solution, the cubic medium is defined in the global coordinate system (Fig. 1) with  $x, y, z \in [0, L]$  and will thereafter be subdivided into many small rectangular hexahedral elements, as described in Sec. III, during the DSEM solution. The medium is initially cold. In the first case, diffuse radiation emits from the bottom wall  $z = 0$  of the cube at  $t = 0$  and then travels in the medium at a finite speed  $c$ . At any given time of  $t$ , the wave front will travel a distance of  $z = ct$  and the dimensionless time of  $t^* = ct/L = z/L$  will give the exact fractional position of the wave front.

The transient incident radiation function (or integrated intensity)  $G(x, y, z, t)$  and the  $z$ -direction transient radiative heat flux  $q_z(x, y, z, t)$  distribution along the centerline of the cube ( $x = 0$ ,  $y = 0$ ) obtained by DSEM for case 1 are presented in Figs. 2a and 2b, respectively. The transient incident radiation function and radiative heat flux of the  $z$  direction is defined and computed as

$$G(x, y, z, t) = \int_0^{2\pi} \int_0^\pi I(x, y, z, t, \theta, \varphi) \sin \theta d\theta d\varphi \quad (8a)$$

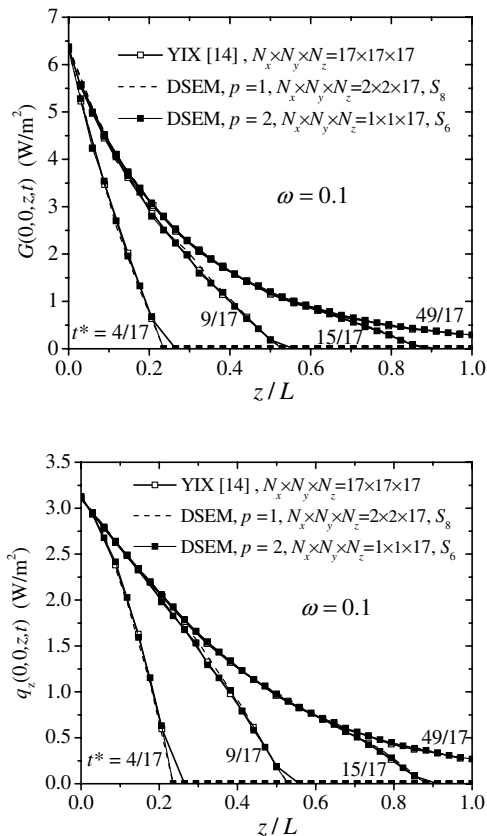


**Fig. 2** Transient incident radiation function and heat flux distribution along the centerline of a cube with one diffusive emission boundary: a) incident radiation function and b) heat flux.

$$q_z(x, y, z, t) = \int_0^{2\pi} \int_0^\pi I(x, y, z, t, \theta, \varphi) \cos \theta \sin \theta d\theta d\varphi \quad (8b)$$

The results obtained using the YIX method [14] (named after the shape of the pattern of the integration points for three, two, and four angular directions) are also shown as a comparison. Here, two mesh decomposition schemes are used for the DSEM: namely,  $N_x \times N_y \times N_z = 2 \times 2 \times 17$  elements in which  $p = 1$  and  $N_x \times N_y \times N_z = 1 \times 1 \times 17$  elements in which  $p = 2$ , where  $N_x$ ,  $N_y$ , and  $N_z$  denote the number of elements (subdivisions) for corresponding dimensions. These two spatial decompositions require comparable computational effort. The angular discretization uses the  $S_N$  approximation [15]. The direct component of diffuse irradiation is discretized into  $N_\theta \times N_\varphi = 60 \times 120$  as equivalent beams by a piecewise constant approximation (PCA) scheme, following the special treatment described in [10]. For the temporal discretization, the dimensionless time step is taken as  $\Delta t^* = 1/34$ . The typical computation time for this case when using a Pentium 4, 1.8 GHz computer is about 30 min. Generally, for different instants in time, the results of the DSEM agree very well with the results of the YIX method [14]. The maximum relative error based on the results of the YIX method is less than 3%. It is seen that the higher-order approximation ( $p = 2$ ) gives better accuracy. Because the DSEM allows discontinuities at the element boundary, it ensures accurate prediction of the wave front when it is located on the element boundary. This characteristic of the DSEM agrees well with the examination conducted in one and two dimensions [10].

In the second case, the DSEM is applied to model transient radiative transfer in an anisotropically scattering medium. The scattering phase function of the medium is  $\Phi(\mathbf{\Omega}, \mathbf{\Omega}') = 1 + a \mathbf{\Omega} \cdot \mathbf{\Omega}'$ . For  $a = -1, 0$ , and  $1$ , the phase function is backward, isotropic, and forward scattering, respectively. The transient incident radiation and the radiative heat flux distribution along the centerline of the cube ( $x = 0$ ,  $y = 0$ ), obtained by the DSEM for case 2, are shown in Figs. 3a and 3b, respectively. The cube is decomposed into  $N_x \times N_y \times N_z = 2 \times 2 \times 17$  elements in which  $p = 2$  for the spectral element approximation. The angular discretization is by the  $S_6$  approximation. The direct component of diffuse irradiation is discretized into  $N_\theta \times N_\varphi = 160 \times 80$  equivalent beams by the PCA scheme. The DSEM accurately predicts the wave front at different instants of time. Compared with isotropic scattering, forward scattering significantly enhances heat flux, which is the opposite for backward scattering. This is reasonable because more energy emitted from the bottom wall is scattered upward (in the positive  $z$  direction) for forward scattering, and vice versa for backward scattering. The effect of different phase functions on the incident radiation results in more complex behavior. At a given instant in time, both enhancement and weakening happens in the incident radiation curve.

A collimated beam propagating through a purely isotropic scattering medium of three different optical thicknesses (namely,  $\tau_L = 0.1, 1$ , and  $2$ ) is considered in the third case. The beam enters the bottom wall of the cube and transmits in the  $z$  direction. The transient incident radiation and the radiative heat flux distribution along the centerline of the cube ( $x = 0$ ,  $y = 0$ ) obtained by the DSEM for case 3 are shown in Figs. 4a and 4b, respectively. In this study, the cube is divided into  $N_x \times N_y \times N_z = 4 \times 4 \times 10$  elements in which  $p = 2$  for the spectral element approximation. The angular discretization uses the  $S_8$  approximation. The dimensionless time step is taken as  $\Delta t^* = 0.02$ . Here, the dimensionless time  $t^*$  gives the position of the wave front, as was the situation for the former cases.

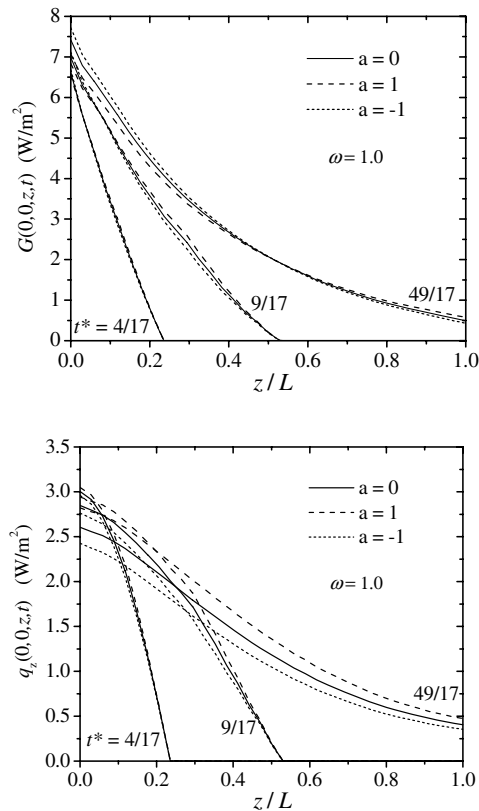


**Fig. 3** Transient incident radiation function and heat flux distribution along the centerline of a cube filled with linear anisotropic-scattering medium: a) incident radiation function and b) heat flux.

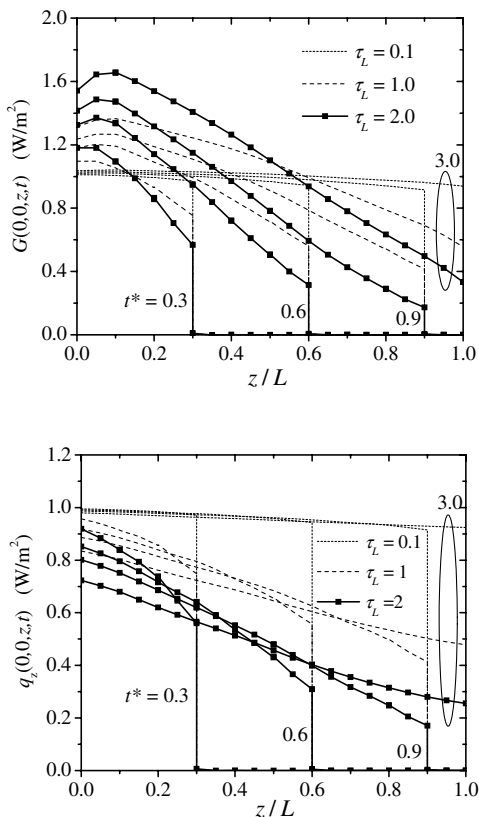


**Fig. 4** Transient incident radiation function and heat flux distribution along the centerline of a cube with one collimated intensity emitting boundary: a) incident radiation function and b) heat flux.

The DSEM accurately predicts the transient sharp wave fronts for different instants in time. With increasing optical thickness, the scattering effect is enhanced. A peak appears in the incident radiation curve at each instant in time. The position of maximum incident radiation is not at the bottom wall, due to the scattering contribution. At each instant in time, the heat flux distribution monotonically decreases with increasing optical thickness. The DSEM shows very good performance in solving a transient collimated beam radiative transfer problem and can accurately capture the sharp wave fronts.

## V. Conclusions

DSEM is presented to solve transient radiative transfer problems in a three-dimensional semitransparent medium. The performance of the DSEM in modeling three-dimensional transient radiative transfer processes is examined. The predictions of the DSEM agree well with reported solutions in the literature. The DSEM is demonstrated to be efficient and accurate in capturing the sharp wave fronts of a transient radiative transfer process. Because of high accuracy of spatial discretization, accurate results can be obtained by DSEM with relatively few elements.

## Acknowledgments

The support of this work by the National Nature Science Foundation of China (50636010, 50620120442) is gratefully acknowledged. The authors thank Ronald L. Dougherty for his careful reading and warmhearted help in improving the English text and the quality of this paper.

## References

- [1] Kumar, S., and Mitra, K., "Microscale Aspects of Thermal Radiation Transport and Laser Application," *Advances in Heat Transfer*, Vol. 33, 1999, pp. 187–294.
- [2] Yamada, Y., "Light-Tissue Interaction and Optical Imaging in Biomedicine," *Annual Review of Heat Transfer*, Vol. 6, 1995, pp. 1–59.
- [3] Nussbaum, E. L., Baxter, G. D., and Lilge, L., "A Review of Laser Technology and Light-Tissue Interactions as a Background to Therapeutic Applications of Low Intensity Lasers and Other Light Sources," *Physical Therapy Reviews*, Vol. 8, No. 1, 2003, pp. 31–44. doi:10.1179/108331903225001381
- [4] Guo, Z., Kumar, S., and San, K., "Multidimensional Monte Carlo Simulation of Short-Pulse Laser Transport in Scattering Media," *Journal of Thermophysics and Heat Transfer*, Vol. 14, No. 4, 2000, pp. 504–511. doi:10.2514/2.6573
- [5] Tan, Z.-M., and Hsu, P.-F., "An Integral Formulation of Transient Radiative Transfer," *Journal of Heat Transfer*, Vol. 123, No. 3, 2001, pp. 466–475. doi:10.1115/1.1371230
- [6] Guo, Z., and Kumar, S., "Discrete-Ordinates Solution of Short-Pulsed Laser Transport in Two-Dimensional Turbid Media," *Applied Optics*, Vol. 40, No. 19, 2001, pp. 3156–3163. doi:10.1364/AO.40.003156
- [7] Mitra, K., Lai, M.-S., and Kumar, S., "Transient Radiation Transport in Participating Media with a Rectangular Enclosure," *Journal of Thermophysics and Heat Transfer*, Vol. 11, No. 3, 1997, pp. 409–414. doi:10.2514/2.6255
- [8] Chai, J. C., "One-Dimensional Transient Radiation Heat Transfer Modeling Using a Finite-Volume Method," *Numerical Heat Transfer, Part B: Fundamentals*, Vol. 44, No. 2, 2003, pp. 187–208. doi:10.1080/713836346
- [9] Liu, L. H., and Hsu, P.-F., "Analysis of Transient Radiative Transfer in Semitransparent Graded Index Medium," *Journal of Quantitative Spectroscopy and Radiative Transfer*, Vol. 105, No. 3, 2007, pp. 357–376. doi:10.1016/j.jqsrt.2006.12.003
- [10] Zhao, J. M., and Liu, L. H., "Discontinuous Spectral Element Approach for Solving Transient Radiative Transfer Equations," *Journal of Thermophysics and Heat Transfer*, Vol. 22, No. 1, 2008, pp. 20–28. doi:10.2514/1.32688
- [11] Liu, L. H., and Hsu, P.-F., "Time Shift and Superposition Method for Solving Transient Radiative Transfer Equation," *Journal of Quantitative Spectroscopy and Radiative Transfer*, Vol. 109, No. 7,

- 2008, pp. 1297–1308.  
doi:10.1016/j.jqsrt.2007.10.005
- [12] Zhao, J. M., and Liu, L. H., “Least-Squares Spectral Element Method for Radiative Heat Transfer in Semitransparent Media,” *Numerical Heat Transfer, Part B: Fundamentals*, Vol. 50, No. 5, 2006, pp. 473–489.  
doi:10.1080/10407790600682821
- [13] Zhao, J. M., and Liu, L. H., “Discontinuous Spectral Element Method for Solving Radiative Heat Transfer in Multidimensional Semitransparent Media,” *Journal of Quantitative Spectroscopy and Radiative Transfer*, Vol. 107, No. 1, 2007, pp. 1–16.  
doi:10.1016/j.jqsrt.2007.02.001
- [14] Tan, Z.-M., and Hsu, P.-F., “Transient Radiative Transfer in Three-Dimensional Homogeneous and Nonhomogeneous Participating Media,” *Journal of Quantitative Spectroscopy and Radiative Transfer*, Vol. 73, Nos. 2–5, 2002, pp. 181–194.  
doi:10.1016/S0022-4073(01)00221-7
- [15] Fiveland, W. A., “Discrete-Ordinates Solution of the Radiative Transport Equation for Rectangular Enclosures,” *Journal of Heat Transfer*, Vol. 106, No. 4, 1984, pp. 699–706.